Aberystwyth University

Transport and optical gaps and energy band alignment at organic-inorganic interfaces

Evans, D. A.; Vearey-Roberts, Alex Raymond; Roberts, O. R.; Williams, G. T.; Cooil, S. P.; Langstaff, D. P.; Cabailh, G.; McGovern, I. T.; Goss, J. P.

CrossMark
click for updates

Transport and optical gaps and energy band alignment at organic-inorganic interfaces

D. A. Evans,[1,a)] A. R. Vearey-Roberts,[1] O. R. Roberts,[1,b)] G. T. Williams,[1,c)] S. P. Cooil,[1] D. P. Langstaff,[1] G. Cabailh,[2,d)] I. T. McGovern,[2] and J. P. Goss[3]

[1]*Department of Mathematics and Physics, Aberystwyth University, Aberystwyth SY23 3BZ, United Kingdom*
[2]*Department of Physics, Trinity College, Dublin 2, Ireland*
[3]*School of Electrical, Electronic and Computer Engineering, Newcastle University, Newcastle upon Tyne NE1 7RU, United Kingdom*

The transport and optical band gaps for the organic semiconductor tin (II) phthalocyanine (SnPc) and the complete energy band profiles have been determined for organic-inorganic interfaces between SnPc and III-V semiconductors. High throughput measurement of interface energetics over timescales comparable to the growth rates was enabled using *in situ* and real-time photoelectron spectroscopy combined with Organic Molecular Beam Deposition. Energy band alignment at SnPc interfaces with GaAs, GaP, and InP yields interface dipoles varying from -0.08 (GaP) to -0.83 eV (GaAs). Optical and transport gaps for SnPc and CuPc were determined from photoelectron spectroscopy and from optical absorption using spectroscopic ellipsometry to complete the energy band profiles. For SnPc, the difference in energy between the optical and transport gaps indicates an exciton binding energy of (0.6 ± 0.3) eV. © *2013 AIP Publishing LLC*. [http://dx.doi.org/10.1063/1.4823518]

I. INTRODUCTION

In many applications exploiting the electronic,[1] energy harvesting,[2] spintronic,[3] and bio-sensing[4] properties of multi-component structures based on conjugated organic conductors, the performance-limiting factor is often the energy band alignment at hetero-interfaces. For example, organic photovoltaics depend on a band edge discontinuity to dissociate the excitons generated by light absorption and this interface parameter is not always reliably predicted theoretically or using bulk material properties.[2] Charge transfer and polarization are commonly induced during heterointerface formation even in van der Waals-bonded systems resulting in dipole layers and band-bending that must be considered in the overall energy band picture.[5]

Few experimental methods can provide all the interface energy parameters and fewer still can be applied *in situ* during fabrication. Here, we show how the complete energy band profile for an organic-inorganic interface can be determined *in situ* and in real time using the single technique of photoelectron spectroscopy. *In situ* measurement ensures accurate determination of energy values and real-time measurement provides the evolution of band offsets and band bending as the interface is formed in addition to the interface chemistry and thin film morphology. The interface parameters are found to evolve at different rates during growth and

this has important consequences for device design and operation.

The most direct methods for probing electronic states in solid materials involve photo-excitation of electrons using electromagnetic radiation resonant with initial and/or final state energies. Optical sources probe states within and around the band gap and larger energy UV and X-ray sources induce additional transitions from deeper core states. Refinement of techniques based on reflection, absorption, and emission of radiation and electrons is driven by a need to better understand increasingly complex materials systems. Among these techniques, photoelectron spectroscopy is perhaps the most direct and versatile in that it probes both bonding and core states providing chemical, electronic and in some cases morphological and structural information in a single method. As an *in situ* materials characterization technique, it does, however, have limitations in comparison with optical and electrical methods in that it conventionally requires a vacuum environment and can be complex, expensive, and slow. Nevertheless, such is the quality of information available that considerable effort has been applied to enable *in situ* measurement of, for example, ambient pressure adsorbates on semiconductors,[6] oxidation of surfaces,[7] and high temperature interfaces.[8]

We have applied this approach to the fabrication of organic-inorganic semiconductor interfaces in a modified Organic Molecular Beam Deposition (OMBD) system that enables *in situ* and real-time characterization of molecular adsorption and incorporation into the evolving thin films. By selecting appropriate incident photon energies, both core and valence states are probed sequentially to provide parallel chemical and electronic information. This method has been applied to probe chemical and structural changes during the adsorption of monolayers (MLs),[9] inorganic films,[10] and

---

a)Author to whom correspondence should be addressed. Electronic mail: a.evans@aber.ac.uk
b)Current address: Element Six Ltd, Global Innovation Centre, Didcot, OX11 0QR, United Kingdom
c)Current address: National Library of Wales, Aberystwyth, SY23 3BU, United Kingdom
d)Current address: Institut des Nanosciences de Paris, 75252 Paris cedex 05, France

organic films[11] and here is applied to determine the energetics of semiconductor interfaces.

The aim of this study was to obtain the complete energy band profile of organic-inorganic interfaces using, as an example, the growth of metal phthalocyanine thin films on III-V semiconductor surfaces. The optical properties of phthalocyanines (e.g., tin(II) phthalocyanine (SnPc)) are exploited in efficient organic photovoltaic cells,[12] and the electronic properties of phthalocyanine-III-V interfaces feature in novel spin valves[13] and in modified Schottky diodes.[14]

For organic semiconductors, parameters such as the energy band gap are not as well defined as for their inorganic counterparts. The band gap is usually taken as the highest occupied molecular orbital (HOMO)-lowest unoccupied molecular orbital (LUMO) separation derived from optical absorption measurements. However, this does not uniquely define this parameter as simply as for inorganic semiconductors due to the generation of a Frenkel exciton during the optical absorption process.[15] Because of the weak screening and strong electron-hole coulomb interaction, the band gap determined by optical absorption can be significantly less than the transport gap, with the difference related to the exciton binding energy that can be a significant fraction of the HOMO-LUMO gap.[16] A correlation has been found between the magnitude of the exciton binding energy and the size of the excited molecule for a number of π-conjugated molecules.[17]

It is important, therefore, to measure both the transport and optical band gaps to determine the exciton binding energy. The transport gap can be measured using the photoconductivity of the organic film[18] and by a combination of direct and inverse photoelectron spectroscopy.[16,19] For copper phthalocyanine (CuPc) thin films, it has been found that the exciton binding energy is (0.6 ± 0.4) eV,[16] a typical value for such films of ordered small conjugated molecules. A further factor for organic semiconductor interfaces with metals or inorganic semiconductors is a change in polarization that can lead to a transport gap at the surface that can be larger than the bulk gap. Here, we show how both optical and transport gaps can be derived using *in situ* and real-time photoelectron spectroscopy to complete the energy band profile for organic-inorganic semiconductor interfaces.

II. EXPERIMENTAL

Substrate surfaces were prepared by chemically etching epi-ready (001)-oriented wafers of GaAs, GaP and InP using dilute (0.1M) sulfur monochloride to produce partially passivated, S-terminated surfaces.[20] Ohmic back contacts were prepared on the reverse of all samples prior to insertion into the OMBD/analysis environment. Following *in situ* annealing to 450 °C to remove excess sulfur, ordered and oxygen-free surfaces were confirmed by photoelectron spectroscopy and the observation of characteristic 2×1 Low Energy Electron Diffraction (LEED) patterns. A consistent separation of $(0.2–0.4)$ eV for the valence band edges for n- and p-type materials relative to a reference metal Fermi level resulted from partial electronic passivation of the surfaces.

Organic films were grown onto these surfaces by collimated evaporation from Knudsen cells calibrated using a

quartz crystal oscillator placed close to the analysis position. Photoelectron spectroscopy measurements were undertaken using Mg Kα, He I, and soft x-ray synchrotron radiation. In all cases, photoelectrons were energy analyzed using a hemispherical analyzer coupled to a direct electron-counting array detector.[21] This device has 768 detection channels that enable segments of the electron distribution curve (~ 6 eV) to be recorded in around 2 s per spectrum using conventional x-ray and UV sources and around 100 ms using synchrotron radiation. The ideal arrangement for monitoring growth involves selecting a photon energy that allows substrate and overlayer core levels (e.g., Ga3d, As3d, and Sn4d) and the band edges to be measured rapidly and sequentially with optimal surface sensitivity. The overall recording time for such a sequence was adequate for real-time monitoring of SnPc at growth rates of around $(0.01–1)$ nm min^{-1}. The dynamic range of the array detector enabled detection of both intense and weak features without changing the operating voltage of the multichannel plate. Photoelectron spectra were corrected for detector uniformity and incident flux intensity and each spectrum was curve-fitted to extract peak positions and intensities. Data for many growth runs were accumulated and compared.

Optical absorption in SnPc films was measured using a variable-angle spectroscopic ellipsometer (Sopra Ltd) with a Xe white light source to provide an estimate of the optical band gap and higher HOMO-LUMO transitions. Density functional theory (DFT) calculations were performed for isolated SnPc molecules to determine their degree of nonplanarity and to provide the electron density distribution of the HOMO and LUMO orbitals.

III. RESULTS AND DISCUSSION

A. Real-time photoelectron spectroscopy

The experimental approach is shown schematically in Figure 1(a). Incident radiation excites photoelectrons in the near-surface region that are collected continuously during the growth of the organic layer. The surface sensitivity is determined by the electron energy and, for a given core or valence state, this can be varied by the choice of incident photon energy. This is illustrated in Figure 1(b) by the
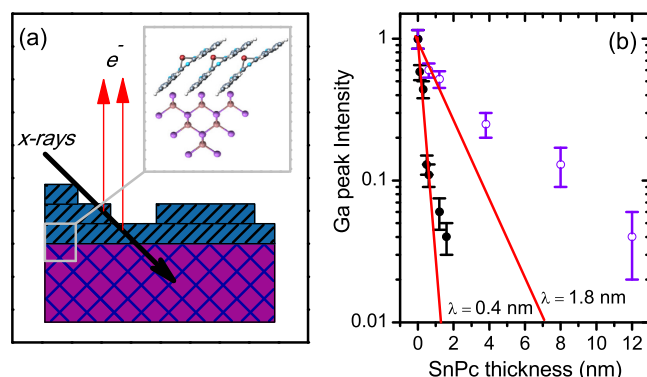

FIG. 1. (a) Schematic of SnPc growth on S:GaAs(001). The first layer is uniform with molecules arranged at an angle of 39° with respect to the substrate. Subsequent layers are more clustered. (b) Attenuation of the Ga3d photoemission peak intensity for incident photon energies of 105 eV (solid symbols) and 1253 eV (open symbols) recorded in conventional mode.

attenuation of the substrate (Ga3d) photoelectron peak intensity for a GaAs(001) surface exposed to SnPc.

The attenuation rate for photoelectrons excited by a laboratory x-ray source (open symbols) is slower than for photoelectrons excited by a lower energy synchrotron radiation source (solid symbols) due to the different surface sensitivity (the electron escape depth for the laboratory x-ray source is 1.8 nm, compared with an escape depth of 0.4 nm for the synchrotron x-ray source). The lower energy x-rays are, therefore, preferable for studies of ML growth, while the higher energies are better suited for studies of thicker films. In both cases, there is a point of inflection in the attenuation curve at a thickness of around 1 nm.

The data in Figure 1(b) were collected in conventional scanned mode using channeltron detection, with each experiment taking many hours and necessitating a stop-start growth and measurement sequence. Errors in peak intensity and peak position and the long data collection time introduce considerable and often unacceptable uncertainty in parameters required for an accurate picture of the interface energetics and the time evolution of growth. A real-time, *in situ* method has therefore been applied, as illustrated in Figure 1(a).

For this interface, it has been found that the thickness of the initial uniform layer is 0.9 nm and within this layer, the molecules are aligned at an angle of 39° to the substrate.[11,22]

A sequence of As3d, Ga3d, and Sn4d photoelectron spectra acquired in real-time with a fixed incident photon energy of 105 eV is presented in Figure 2. These data formed part of a set of core and band edge spectra recorded during exposure of the S:GaAs(001) surface to a flux of SnPc, and part of a wider study of metal phthalocyanine growth on a range of substrates, including III-V semiconductors. Snapshot spectra (open symbols) are shown above each time sequence for the three core levels in comparison with higher resolution scanned spectra (closed symbols) and their fitted components (solid lines).

The Ga3d and As3d spectra are typical of the initial surface where the additional Ga components at higher binding energy correspond to two Ga-S bonding sites in the topmost layer, whereas the As atoms are predominantly located within the GaAs bulk.[23] The Sn4d peak was recorded for the final SnPc film and is largely made up of a single doublet corresponding to the Sn^{2+} ion within the SnPc molecule. There is a smaller additional component at higher binding energy corresponding to higher oxidation states; this component is not significant in this case, but can be prominent when probing with higher intensity radiation.[24] The substrate peak components showed little change during exposure (apart from energy broadening) indicating a chemically inert interface[25] and hence the main peak position can be used to monitor changes in the substrate band-bending during interface formation.

Initially, spectra were recorded without powering the cell to confirm beam and spectrometer stability. At t = 500 s (lower dashed horizontal line in Figure 2), the cell power was increased and held at 5 W to provide a constant exposure rate of 0.01 nm (min)$^{-1}$. The cell power was switched off at t = 11 000 s (upper dashed horizontal line in Figure 2) when there were no further changes in peak position and intensity. Spectra were recorded for a further 3500 s to monitor post-growth changes in the substrate and overlayer spectra. The use of soft x-ray excitation enabled all spectra to be recorded with similar probing depth to ensure maximum surface sensitivity (the minimum escape depth of $\lambda = 0.34$ nm was measured for the As3d core level[22]). Bending magnet radiation ensured minimal beam damage during exposure to the synchrotron beam.[24]

Fitting of each spectrum in the sequence yields the bulk peak positions and the energy shift of the Ga3d bulk peak is plotted as a function of time and coverage (for the uniform growth regime) in Figure 3. The time-evolution recorded in real time (large closed symbols) is compared with data recorded conventionally over a longer time period (inset of Figure 3). These data do not match exactly and it appears
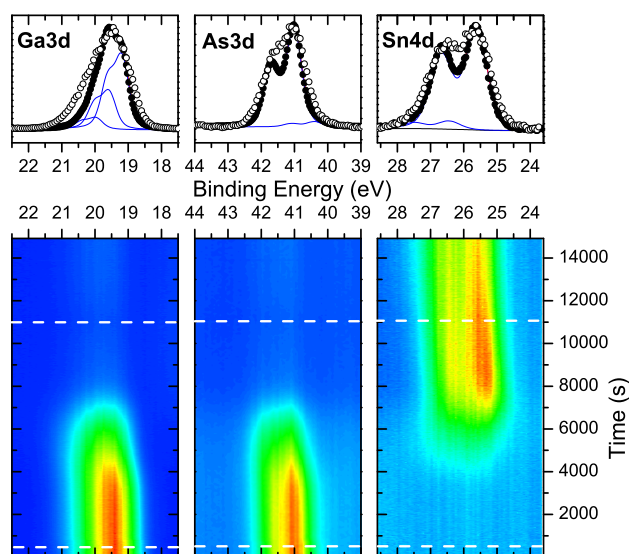

FIG. 2. Real-time core level photoelectron spectra recorded during the growth of SnPc on a GaAs (001) surface. The upper panels show snapshot spectra (open symbols) superimposed on higher resolution scanned spectra and their fitted components. The horizontal lines in the 2-d projected real-time data (lower panels) indicate the start and end of SnPc exposure.
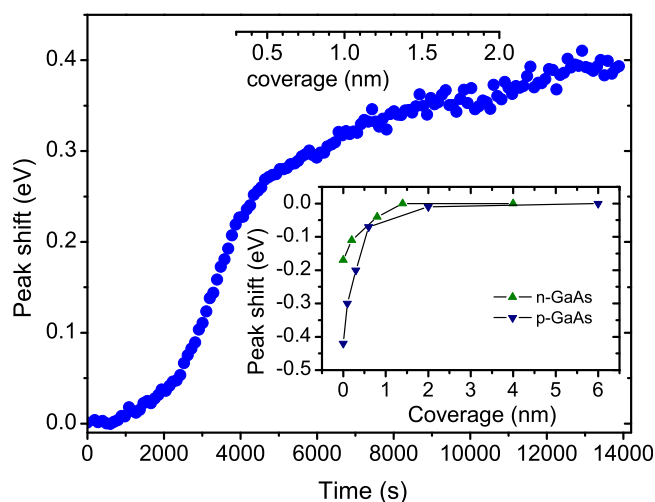

FIG. 3. Substrate Ga3d core level shift before, during, and after exposure of a p-GaAs(001) surface to SnPc. The time/coverage evolution of the real-time data is different to the conventionally recorded data (inset). The SnPc coverage scale, determined from a quartz microbalance calibration, is shown for the region of uniform molecular flux at constant cell power.

that the band-bending changes are linked to the morphological changes occurring at the molecular level over timescales comparable to the growth rates.[11]

The peak shift commences at t = 500 s, long before there is a discernible decrease in peak intensity but continues even beyond the end of exposure to the molecular beam at t = 11 000 s. This is quite unlike the effect of metal overlayers on such substrates where band-bending changes are complete for sub-monolayer levels.[26] The rate of change of peak position is highest when the SnPc film thickness is in the range of 0–0.5 ML, and the final band-bending position is established for organic layers of thickness > 2 nm. It is important, therefore, to consider both the thickness and the time when extracting peak positions from the data, and both can be optimized for fast-throughput characterization of interface energetics using this real-time approach.

A notable feature of the measured peak shifts for n-type and p-type GaAs is that they occur in the same direction. This leads to an increase in the depletion width of p-GaAs while reducing it for n-GaAs. The Fermi level moves close to the conduction band minimum in each case suggesting a common pinning position determined by new interface states generated at the organic–inorganic interface. It has been shown in I-V measurements of modified n-GaAs-SnPc-Ag diodes that this effect persists in the presence of the metal contact resulting in the formation of almost ohmic contacts when the organic interlayer reaches a thickness of 4 nm.[14] It is unusual for GaAs to form simple contacts with barrier heights deviating far from mid-gap[27] and this method offers ways of both increasing and decreasing this important parameter between 0.3 and 1.1 V by changing the thickness of the organic thin film.

In addition to quantifying band-bending changes in the substrate, it is also necessary to identify changes in the evolving organic film. This is illustrated in the time-dependent series of Sn4d core level and band edge spectra recorded in the same experiment as the substrate core level spectra (Figures 2 and 4(a)). There is a discernible Sn4d emission peak at an exposure of 4000 s corresponding to an organic film thickness of 0.3 nm and this grows to saturation at 8000 s corresponding to a thickness of 1.2 nm. At this point, the probing depth of the experiment lies mainly in the bulk of the organic overlayer. The projected 2-d Sn4d data (Figure 2) reveal an energy shift that is different to that for the substrate and hence there must also be a change in the organic energy levels with respect to the Fermi level during thin film growth. Both substrate and overlayer band-bending must, therefore, be considered when formulating the interface band alignment.

B. Interface energetics

Having determined the thickness-dependent energy changes on either side of the interface, the energy band alignment at the interface is obtained by recording band-edge photoelectron spectra during interface formation as shown in Figure 4.

Real-time data collected within 5 eV of the Fermi level (0 eV) in Figure 4(a) show how the valence band maximum
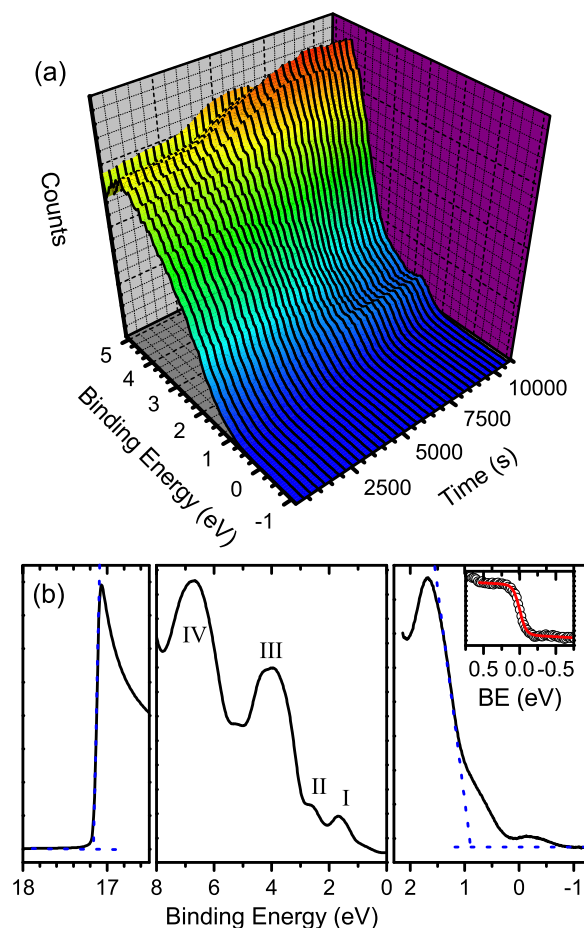

FIG. 4. (a) Real-time evolution of the valence band edge during exposure of a GaAs surface to SnPc. The incident photon energy was 105 eV. (b) Valence band photoelectron spectra for a 4 nm SnPc film on S:GaAs along with the secondary electron emission onset and the magnified band-edge emission near the Fermi level at 0 eV. The secondary electron emission was measured with a sample bias of −5 V. The photoelectrons were excited using He I radiation.

of GaAs evolves into the HOMO emission at the band edge of SnPc during the growth of the interface. The peak at 1.6 eV, corresponding to the HOMO of the organic semiconductor, first appears at 5000 s (0.5 nm) and is fully formed at 8000 s (1.2 nm). Due to the high surface sensitivity, this characterization approach is thus efficient not only in the speed of measurement but also in the small amount of material required in test structures in comparison to the fabrication of entire devices. These real-time measurements inform the selection of organic film thicknesses for further data collection at higher energy resolution to obtain a more accurate picture of the energy band alignment.

The determination of interface energetics from photoelectron spectroscopy requires the measurement of the ionization energy (or work function) in addition to the band edges and band bending. This is needed to deduce the position of the vacuum level with respect to the Fermi level on either side of the junction and can be obtained by recording the low kinetic energy onset of the photoelectron spectrum in addition to the high kinetic energy band edge. Figure 4(b) presents selected band edge and occupied molecular orbital spectra for a 4 nm SnPc film recorded using excitation by a

He I UV source. The valence band spectra, encompassing the density of hybrid s and p states in the substrate and the organic HOMO states, are dominated by overlayer features at coverages above 0.9 nm (around one stacked molecular layer[22]) and the secondary onset is also saturated by this point. The main peaks in the spectrum (I-IV) are shown in Figure 4(b). Most of the spectral features are common for different metal phthalocyanines including PbPc that, like SnPc, has an out-of-plane metal ion.[28] Peaks III and IV have been reported to have both C2p and N2p character.[29,30] The HOMO, peak I, has been identified as a π molecular orbital with strong contributions from the carbon atoms bonded to nitrogen on the macrocycle. Peak II is the most sensitive to the central metal ion: it is not observed in PbPc[28] or Sn(IV)Pc but is present for both SnPc and CuPc.[31] For SnPc, there is a low intensity emission that extends beyond the HOMO maximum to the Fermi level that is also observed for CuPc but not for Sn(IV)Pc; both CuPc and SnPc overlayers induce band bending in III-V substrates, while Sn(IV)Pc does not.

The ionization energies of the GaAs surface and the bulk-like SnPc overlayer were determined from the width of the photoelectron spectra and these were combined with the thickness-dependent band-bending to obtain the energy band profile (energetics) at the interface as illustrated in Figure 5.

For the substrate (Figure 5(a)), the band-edge relative to the Fermi level (E_v) is determined from measurement of a reference metal Fermi level (E_F) and the valence band edge (E_{VBM}), where $E_v = E_F - E_{VBM}$. The ionization energy of the substrate (IE_{sub}) is obtained from the secondary electron onset (E_{se}), the incident photon energy ($h\nu$), and the valence band edge, where $IE_{sub} = h\nu - (E_{se} - E_{VBM})$. The HOMO energy ($E_H$) and ionization energy for the organic film (IE_{org}) are obtained in a similar way to the substrate parameters (Figure 5(b)). During growth, changes in band bending on either side of the junction are obtained from the real-time measurements and the combination of these values enables the band offset (ΔE_V) and the interface dipole (δ) to be determined as shown in Figure 5(b). The conduction band minimum for the inorganic substrate and the LUMO level for the organic overlayer are not directly measured in photoelectron spectroscopy; these are determined using the optical band

gaps. Since the transport and optical gap for the organic semiconductor are very different, the LUMO level is shown as a dotted line in Figure 5, and it is assumed that there is no narrowing of the organic band gap near the interface.

Quantitative interface energetics measured using this method for three different III-V substrates are presented in Figure 6. In each case, there is a reduction in the substrate n-type band bending (and increase in the p-type band-bending) with the Fermi level pinned closer to the conduction band minimum at the buried interface.

In addition to the band edge discontinuity, there is also an offset in the vacuum level at each interface. This energy imbalance has been the subject of much discussion and it is often overlooked when deriving offsets at organic-organic interfaces using alignment of the constituent bulk ionization energies. For interfaces involving small conjugated molecules,[32–34] this offset is common and significant, and is usually ascribed to an interfacial dipole layer at the interface due to, for example, charge transfer across the interface, redistribution of electron density, interface states, or interfacial chemical reaction.

Following the custom for the adsorption and desorption of molecules on metal surfaces, the difference in the vacuum level, or dipole (δ), is positive when the vacuum level is raised by adsorption of the molecule. For SnPc interfaces with III-V semiconductors, δ varies from −0.08 eV for GaP (Figure 6(b)) to −0.83 for GaAs (Figure 6(a)). The resultant energetics for the three substrates are very different with a staggered profile for GaAs and InP and a straddled profile for GaP. The hole injection barrier is smaller than the electron injection barrier in each case and is almost zero for InP (Figure 6(c)).

C. Optical and transport gap

The HOMO-LUMO gap is not normally obtainable in direct photoelectron spectroscopy and diagrams such as Figures 5 and 6 are completed by positioning the LUMO level according to gaps deduced optically[19,35,36] or using probes of unoccupied electron states in addition to occupied states.[16,19] However, it is possible to extract estimates of the
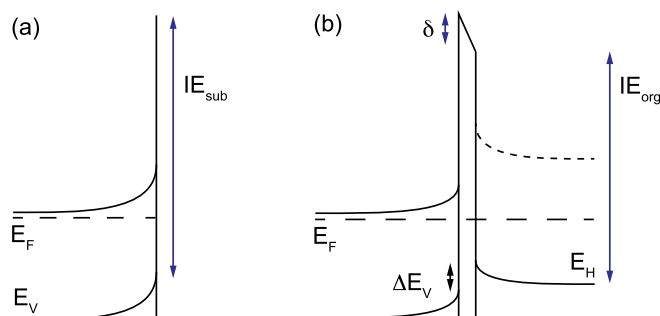
FIG. 5. Energy band diagrams for (a) the S:GaAs(001) surface and (b) the S:GaAs(001)/SnPc interface. Values for the Fermi level (E_F), substrate valence band edge (E_v), the HOMO edge of the organic layer (E_H), and the ionisation energies for each (IE_{sub} and IE_{org}) are obtained from photoelectron spectroscopy measurements. The valence band offset (ΔE_V) and interface dipole (δ) are derived from these measured values.

FIG. 6. Energy band profiles for SnPc heterojunctions with (a) GaAs, (b) GaP, and (c) InP.

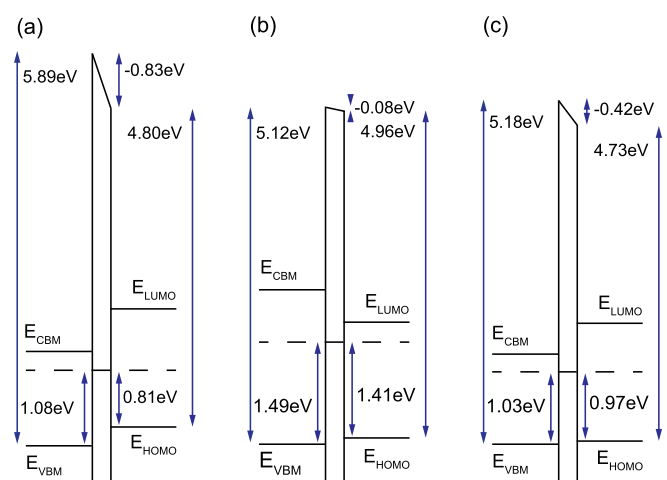band gap from photoelectron spectroscopy if the HOMO-LUMO transitions in organic materials give rise to internal shake-up transitions. Electronic transitions coincident with the main photo-ionization event result in lower kinetic energy satellite peaks in addition to the main photoelectron emission peaks, and these have been reported for many polymers and small organic molecules.[31,37–39] The energy difference between the core level and its associate shake-up satellite provides an estimate of the energy of the internal electronic transition although the absorption/emission process is more complex than that of optical transitions induced by UV/visible/IR photons of energy close to the band gap.

Photoelectron emission spectra for the C1s and N1s core levels in a thin film of SnPc are shown in Figure 7. The minimum number of fit components for the C1s core-level spectrum is four, while only two components are required for the fitting of the N1s spectrum. The results of the fitting are similar to those previously reported for other metal-phthalocyanines.[29,31,39,40] The two main components in the C1s spectrum are due to zero-loss excitations from the core-levels, one due to carbon atoms in the outer benzene ring (C-C/C-H), marked I in Figure 7, and the other due to the carbon atoms in the pyrrole group (C-N), marked II. The other two peaks in the spectrum are the shake-up peaks related to each of the two carbon species. The intensity ratio of the C-N to the C-C components is 3:1 in agreement with the elemental ratio in the SnPc molecule.

The intensity of the C-N shake-up peak relative to the main emission peak is higher than the corresponding relative intensity of the C-C shake-up peak and this can be explained with reference to the calculated charge density for the lowest unoccupied and highest occupied molecular orbitals (Figure 7). These orbitals are more localized on the inner C-N ring and hence a HOMO-LUMO transition is more likely during photo-excitation of carbon atoms located in this part of the molecule than those in the outer benzene rings. The N1s core level spectrum (Figure 7) also contains a shake-up peak at lower kinetic energy, with a lower relative intensity and different energy position in comparison with the C1s components.

The energies of the internal transitions determined from all core level shake-up features are summarized in Table I, along with corresponding measurements for thin films of CuPc prepared in the same way. There is a significant spread in values that are greater than the limits of experimental error (± 0.12 eV). The principal source of uncertainty is the energy resolution and fitting procedure; the values obtained are similar for both SnPc and CuPc. The values are also consistent with those measured by other workers although Cho *et al.* report no difference in energy separation for the 1s components (1.9 eV) for CuPc on ITO.[39] Our data suggest that there is a difference in the energy separation between the satellite peaks and their parents with the largest value (around 2 eV) measured for the C1s C-N component and the smallest (around 1.6 eV) measured for the N1s C-N component.

To allow a comparison between the energy of these internal photoelectron transitions and those induced optically, absorption spectra measured using spectroscopic ellipsometry are shown in Figure 7 for SnPc and CuPc. The spectra are similar for both films with strong absorption at the Q-band at around 1.8 eV and at higher energy bands at around 3.5 eV (B-band) and 4.5 eV (V-band).[36] In films of conjugated polymers and small molecules, the lowest energy $\pi \rightarrow \pi*$ (HOMO-LUMO) transition is usually taken as the maximum of the Q-band[19,41] and these are the values used for the optical gap of SnPc and CuPc in Table I. For SnPc, the maximum has a value of 1.77 eV, while CuPc has a value of 1.72 eV. These are in good agreement with values reported for SnPc in its vapor phase (1.80 eV (Ref. 42)) and in a thin film of α-type SnPc (1.77 eV (Ref. 43)). For CuPc, the Q-band shows a more pronounced splitting, with the shape and energy positions consistent with other ellipsometry measurements (peak maximum at 1.76 eV (Ref. 19)) and with optical absorption measurements (peak maximum at 1.79 eV (Ref. 36)). The shape of the Q-band appears to be
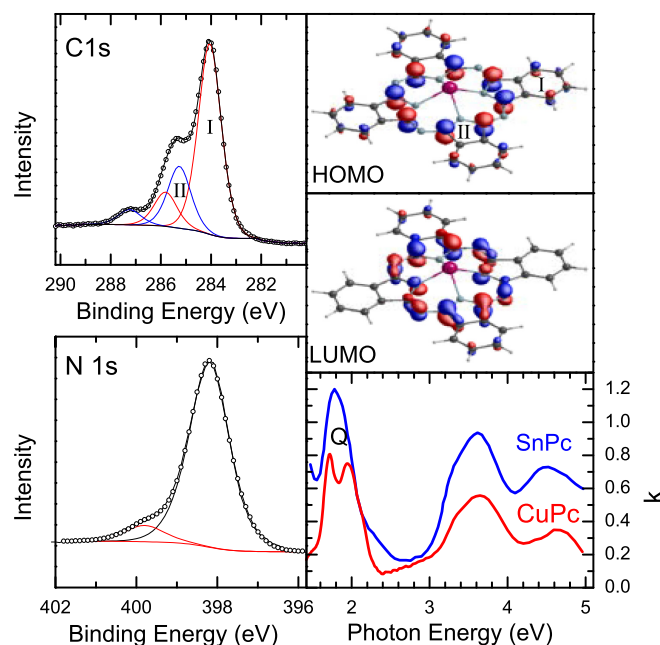

FIG. 7. C1s and N1s core level emission spectra for a SnPc film on GaAs(001) (left hand panels). Hollow circles are the measured data and the solid lines represent the fitted peak components, their shake-up satellites, and the sum of all the components. Calculated molecular orbitals for the LUMO and HOMO states (upper right hand panel) of the isolated molecule reveal stronger localization at the inner pyrrole rings (II) rather than the outer benzene rings (I). The Q-band in the optical absorption spectra of SnPc and CuPc determined by spectroscopic ellipsometry (lower right panel) provides the optical band gap.

TABLE I. Relative peak shifts for the main components and shake-up satellites for the C1s and N1s core level photoelectron spectra and the optical band gaps for SnPc and CuPc.

Energy (eV)	SnPc	CuPc
C1s (C-C)	0	0
Shake-up (C-C)	−1.76	−1.79
C1s (C-N)	−1.21	−1.23
Shake-up (C-N)	−1.99	−2.09
N1s	0	0
Shake-up	−1.59	−1.55
Optical band gap	1.78	1.72

more sensitive to the central metal ion than the higher energy bands; this is a general observation for metal phthalocyanines[19] and is consistent with valence band photoelectron spectroscopy where the states closest to the Fermi level show most sensitivity to the metal ion.

It is perhaps surprising that the shake-up energies are close to the values determined optically since in photoemission, the final state involves a core hole in addition to the exciton. The C1s shake-up components are close to the Q-band energies for SnPc and CuPc, although all are consistently around 0.1 eV higher. The N1s shake-up component is somewhat lower and may be associated with a lower intensity optical transition associated with the low energy shoulder in optical absorption spectra. For example, Farag reports a band-gap of 1.55 eV for CuPc based on optical absorption measurements of thin films on quartz.[36]

Within the experimental uncertainty, the energy position of the shake-up components relative to the main peaks is closer to the optical band gap energies than the transport gap energies. The transport gap can be determined using a combination of photoelectron spectroscopy and inverse photoelectron spectroscopy and is found for films of conjugated organic molecules to be significantly larger than the optical gaps. For CuPc, values of 2.2 eV (Ref. 16) and 2.3 eV (Ref. 19) in comparison to optical gaps of 1.72 eV and 1.78 eV (Table I). This corresponds to an exciton binding energy for both molecules of around 0.6 eV. Similar values have been measured for other phthalocyanine and perylene derivatives.[16,19] Cho *et al.*, in a core level photoelectron spectroscopy study of CuPc on ITO, reported a C1s shake-up energy of 1.9 eV and ascribed this to the transport gap rather than the optical gap.[39] Our data suggest a closer alignment with the optical gaps, especially for the shake-up peak associated with N1s core level and main C-C component of the C1s core level. There remains, therefore, some doubt due to the spreads and uncertainties in the measured values, and it is possible that the measured shake-up peaks are associated with different internal transitions. There is clearly a need to improve the accuracy of photoelectron spectroscopy measurements, for example, using higher energy resolution, improved instrumentation and real-time measurement.

A further method for determining the transport gap using photoelectron spectroscopy is possible when energetics data are available for molecular films on different substrates. Park *et al.* studied Perylene-3,4,9,10-tetracarboxylic dianhydride (PTCDA) films on differently treated n-GaAs surfaces[34] and proposed that the measured interface dipoles can be used to determine the transport gap. The dipole energies were calculated from the difference in the measured electron affinities of the substrate and the organic overlayer ($\Delta\chi = \chi_{sub} - \chi_{org}$), and these were plotted against χ_{sub} for the range of substrates. The transport gap is then determined by extrapolating this linear relationship to $\delta = 0$.

The interface dipoles calculated for the SnPc interfaces with III-V semiconductors measured here (Figure 6) are plotted against the substrate electron affinity χ_{sub} in Figure 8. The dipole is linearly dependent on χ and extrapolation of the linear fit to the data yields $\chi_{sub} = 2.45$ eV for $\delta = 0$ eV. If $\Delta\chi$ is the driving mechanism for the dipole formation, then
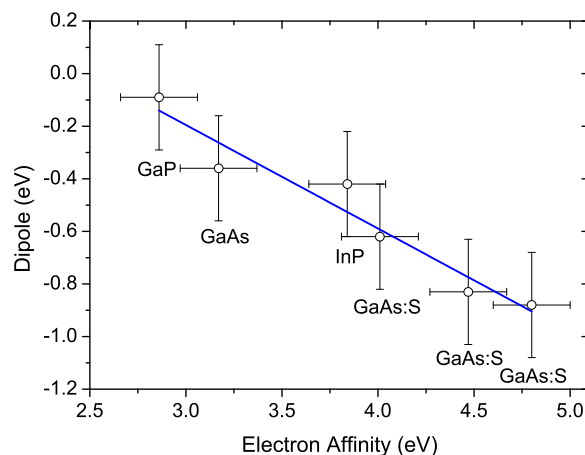

FIG. 8. Interface dipoles calculated for SnPc junctions with n-type III-V semiconductors as a function of measured electron affinity of the substrates. The electron affinity extrapolates to 2.45 eV when the interface dipole = 0.

$\chi_{sub} = \chi_{org}$ when $\delta = 0$ eV. This provides a value for the electron affinity for the SnPc, $\chi_{SnPc} = 2.45$ eV from which the LUMO energy can be deduced. Assuming that the energy levels of the SnPc films extend up to the interface without energy shifts the transport (HOMO-LUMO) gap can be estimated to lie in the range of 2.3 eV to 2.5 eV.

Taking the transport gap to be (2.4 ± 0.2) eV and the optical gap for SnPc to be 1.8 eV (Ref. 35) leads to an exciton binding energy of (0.6 ± 0.3) eV. This value is similar to that reported for metal phthalocyanines and other small conjugated molecular films.[44] The transport gap for SnPc measured here is significantly larger than the shake-up energies in the core level spectra (Table I) and hence our data suggest that the latter are a closer estimate of the optical gap than the transport gap. An even higher value for the transport gap (3.4 eV) has been reported by Walzer and Hietschold in a scanning tunneling spectroscopy study of a single monolayer of SnPc on HOPG.[45] This discrepancy could be due to the measurement methodology or the different growth conditions. For the PTCDA/S:GaAs interface,[46] a similar band gap difference was attributed to the interaction between the STM tip and the organic layer and it was also found that the magnitude of the measured band gap was sensitive to the tip-substrate distance.

Inclusion of the transport gap in the energy diagrams for SnPc on GaAs, GaP, and InP leads to some important consequences. For GaAs and InP, there is an increase in the electron transport barrier, while for GaP there is a closer alignment of both band edges. This junction, therefore, offers a new and efficient injection method for both holes and electrons.

IV. CONCLUSIONS

Complete energy band profiles for organic-inorganic interfaces have been determined using a single *in situ* and real-time method by combining photoelectron spectroscopy with organic molecular beam deposition. SnPc adsorption and incorporation into thin films on III-V semiconductor surfaces result in the formation of chemically inert but electronically active interfaces where the organic film induces

band bending in both n-type and p-type (001) single crystals that have been partially passivated by S-termination. For p and n GaAs, a pinning position for the Fermi level close to the conduction band of GaAs explains the formation of ohmic contacts for GaAs-Ag diodes modified with thin SnPc interlayers and offers the ability to locate the Fermi level at any point between mid-gap and the band edge for both doping types, controlling the barrier in GaAs diodes using the entire band gap. Real-time measurements reveal a slow evolution of the band bending over timescales comparable to molecule arrangement within the films and to the organic semiconductor growth rates. For SnPc interfaces with GaAs, GaP, and InP, energy band alignment results in band offsets that are not determined by alignment of bulk ionization energies of the organic and inorganic materials. This results in the presence of interface dipoles of between $-0.08\,\mathrm{eV}$ (for GaP) and $-0.83\,\mathrm{eV}$ (for GaAs). Both optical and transport gaps have been determined from core and valence level spectra to provide the complete interface energetics and their energy difference indicates an exciton binding energy of $(0.6 \pm 0.3)\,\mathrm{eV}$ for this organic semiconductor.

ACKNOWLEDGMENTS

[1]H. Ohta, T. Kambayashi, K. Nomura, M. Hirano, K. Ishikawa, H. Takezoe, and H. Hosono, Adv. Mater. **16**, 312–316 (2004).

[2]E. L. Ratcliff, B. Zacher, and N. R. Armstrong, J. Phys. Chem. Lett. **2**, 1337–1350 (2011).

[3]V. A. Dediu, L. E. Hueso, I. Bergenti, and C. Taliani, Nature Mater. **8**, 707–716 (2009).

[4]A. Zarbakhsh, M. Campana, D. Mills, and J. R. P. Webster, Langmuir **26**, 15383–15387 (2010).

[5]E. V. Tsiper, Z. G. Soos, W. Gao, and A. Kahn, Chem. Phys. Lett. **360**, 47–52 (2002).

[6]G. Ketteler, S. Yamamoto, H. Bluhm, K. Andersson, D. E. Starr, D. F. Ogletree, H. Ogasawara, A. Nilsson, and M. Salmeron, J. Phys. Chem. C **111**, 8278–8282 (2007).

[7]E. Yoshiharu, S. M. Bongjin, R. Massimiliano, P. N. Ross, Jr., H. Zahid, S. F. Charles, L. Ki-Suk, and K. Sang-Koog, Appl. Phys. Lett. **92**, 012110 (2008).

[8]D. A. Evans, O. R. Roberts, A. R. Vearey-Roberts, D. P. Langstaff, D. J. Twitchen, and M. Schwitters, Appl. Phys. Lett. **91**, 132114 (2007).

[9]A. Baraldi, G. Comelli, S. Lizzit, M. Kiskinova, and G. Paolucci, Surf. Sci. Rep. **49**, 169–224 (2003).

[10]F. Maeda, Y. Watanabe, and M. Oshima, Phys. Rev. Lett. **78**(22), 4233–4236 (1997).

[11]D. A. Evans, O. R. Roberts, A. R. Vearey-Roberts, G. T. Williams, A. C. Brieva, and D. P. Langstaff, Appl. Phys. Lett. **102**, 021605 (2013).

[12]N. Li, B. E. Lassiter, R. R. Lunt, G. Wei, and S. R. Forrest, Appl. Phys. Lett. **94**, 023307 (2009).

[13]H. Ding, Y. Gao, M. Cinchetti, J.-P. Wustenberg, M. Sanchez-Albaneda, O. Andreyev, M. Bauer, and M. Aeschlimann, Phys. Rev. B **78**, 075311 (2008).

[14]A. R. Vearey-Roberts and D. A. Evans, Appl. Phys. Lett. **86**, 072105 (2005).

[15]N. S. Sariciftci, *Primary Photoexcitations in Conjugated Polymers: Molecular Excitation versus Semiconductor Band Model* (World Scientific Publishing Co., 1997).

[16]I. G. Hill, A. Kahn, Z. G. Soos, and R. A. Pascal, Chem. Phys. Lett. **327**, 181–188 (2000).

[17]M. Knupfer, J. Fink, E. Zojer, G. Leising, and D. Fichou, Chem. Phys. Lett. **318**, 585–589 (2000).

[18]R. G. Kepler, J. M. Zeigler, L. A. Harrah, and S. R. Kurtz, Phys. Rev. B **35**, 2818 (1987).

[19]D. R. T. Zahn, G. N. Gavrila, and M. Gorgoi, Chem. Phys. **325**, 99–112 (2006).

[20]D. N. Gnoth, D. Wolfframm, A. Patchett, S. Hohenecker, D. R. T. Zahn, A. Leslie, I. T. McGovern, and D. A. Evans, Appl. Surf. Sci. **123**, 120–125 (1998).

[21]D. P. Langstaff, A. Bushell, T. Chase, and D. A. Evans, Nucl. Instrum. Methods **238**, 219–223 (2005).

[22]D. A. Evans, A. R. Vearey-Roberts, O. R. Roberts, A. C. Brieva, A. Bushell, G. T. Williams, D. P. Langstaff, G. Cabailh, and I. T. McGovern, J. Vac. Sci. Technol. B **28**, C5F5–C5F11 (2010).

[23]G. Hirsch, P. Kruger, and J. Pollmann, Surf. Sci. **402–404**, 778–781 (1998).

[24]G. Cabailh, J. W. Wells, I. T. McGovern, A. R. Vearey-Roberts, A. Bushell, and D. A. Evans, Appl. Surf. Sci. **234**, 144–148 (2004).

[25]A. R. Vearey-Roberts, H. J. Steiner, S. Evans, I. Cerrillo, J. Mendez, G. Cabailh, S. O'Brien, J. W. Wells, I. T. McGovern, and D. A. Evans, Appl. Surf. Sci. **234**, 131–137 (2004).

[26]D. A. Evans, G. J. Lapeyre, and K. Horn, Phys. Rev. B **48**, 1939–1942 (1993).

[27]E. H. Rhoderick and R. H. Williams, *Metal-Semiconductor Contacts* (Clarendon Press, Oxford, 1988).

[28]N. Papageorgiou, Y. Ferro, E. Salomon, A. Allouche, J. M. Layet, L. Giovanelli, and G. Le Lay, Phys. Rev. B **68**, 235105 (2003).

[29]L. Giovanelli, H. Von Schenck, M. Sinner-Hettenbach, N. Papageorgiou, M. Gothelid, and G. Le Lay, Surf. Sci. **486**, 55–64 (2001).

[30]E. Tegeler, M. Iwan, and E. E. Koch, J. Electron Spectrosc. Relat. Phenom. **22**, 297 (1981).

[31]D. A. Evans, H. J. Steiner, S. Evans, R. Middleton, T. S. Jones, S. Park, T. U. Kampen, D. R. T. Zahn, G. Cabailh, and I. T. McGovern, J. Phys.: Condens. Matter **15**, S2729–S2740 (2003).

[32]H. Ishii, K. Sugiyama, E. Ito, and K. Seki, Adv. Mater. **11**, 605 (1999).

[33]I. G. Hill, A. Rajagopal, A. Kahn, and Y. Hu, Appl. Phys. Lett. **73**, 662–664 (1998).

[34]S. Park, T. U. Kampen, D. R. T. Zahn, and W. Braun, Appl. Phys. Lett. **79**, 4124–4126 (2001).

[35]Y. L. Pan, L. B. Chen, Y. Wang, Y. Y. Zhao, F. M. Li, H. W. Zhou, A. Wagiki, M. Yamashita, and T. Tako, Appl. Phys. A **65**, 425–428 (1997).

[36]A. A. M. Farag, Opt. Laser Technol. **39**, 728–732 (2007).

[37]S. A. Chambers and T. D. Thomas, J. Chem. Phys. **67**, 2596–2603 (1977).

[38]R. Nakagaki, D. C. Frost, and C. A. McDowell, J. Electron Spectrosc. Relat. Phenom. **27**, 69–73 (1982).

[39]S. W. Cho, L. F. J. Piper, A. DeMasi, A. R. H. Preston, K. E. Smith, K. V. Chauhan, R. A. Hatton, and T. S. Jones, J. Phys. Chem. C **114**, 18252–18257 (2010).

[40]A. Ruocco, M. P. Donzello, F. Evangelista, and G. Stefani, Phys. Rev. B **67**, 155408 (2003).

[41]L. S. Liao, M. K. Fung, C. S. Lee, S. T. Lee, M. Inbasekaran, E. P. Woo, and W. W. Wu, Appl. Phys. Lett. **76**, 3582–3584 (2000).

[42]D. Dini and M. Hanack, *The Porphyrin Handbook* (Elsevier Science, 2003).

[43]Y. L. Pan, L. B. Chen, Y. Wang, Y. Y. Zhao, F. M. Li, A. Wagiki, M. Yamashita, and T. Tako, Appl. Phys. Lett. **68**, 1314–1316 (1996).

[44]I. G. Hill, A. Kahn, J. Cornil, D. A. dos Santos, and J. L. Bredas, Chem. Phys. Lett. **317**, 444–450 (2000).

[45]K. Walzer and M. Hietschold, Surf. Sci. **471**, 1–10 (2001).

[46]N. Nicoara, O. Custance, D. Granados, J. M. Garcia, J. M. Gomez-Rodriguez, A. M. Baro, and J. Mendez, J. Phys.: Condens. Matter **15**, S2619–S2629 (2003).